Available online at www.sciencedirect.com
ScienceDirect
Electrochemistry Communications 9 (2007) 1525–1529
electrochemistry communications
www.elsevier.com/locate/elecom

Nanozeolite-assembled interface towards sensitive biosensing

Xiaoqin Zhou [a], Tao Yu [a], Yahong Zhang [a,*], Jilie Kong [a], Yi Tang [a], Jean-Louis Marty [b], Baohong Liu [a,*]

[a] Department of Chemistry and Shanghai Key Laboratory of Molecular Catalysis and Innovative Materials, Fudan University, Shanghai 200433, PR China
[b] BIOMEM, University of Perpignan Via Domitia, 66860 Perpignan, France

Received 29 January 2007; received in revised form 12 February 2007; accepted 19 February 2007
Available online 23 February 2007

Abstract

A biocompatible surface has been constructed on the electrode surface via layer-by-layer assembly of beta-nanozeolites and polydiallyldimethylammonium (PDDA) for the adsorption of enzymes towards sensitive biosensing. The film assembly process and enzyme adsorption were monitored by Quartz Crystal Microbalance measurements. The nanozeolite film exhibited an amazing adsorption capacity (about 350 mg g^{-1}) for tyrosinase as a model enzyme. The tyrosinase biosensor showed a high sensitivity (400 μA mM^{-1}), short response time (reaching 95% within 5 s), broad linear response range from 10 nM to 18 μM, very low detection limit (0.5 nM) and high operational and storage stability (more than 2 months). The apparent Michaelis–Menten constant K_M^{app} was calculated to be 24 μM using phenol as the substrate. The assembly-controlled nanozeolite film could provide a biocompatible surface for the interaction study between enzymes and target molecules.

Keywords: Nanozeolite; Layer-by-layer; Biointerface; Electrochemistry; Sensor

1. Introduction

Surfaces play an important role in biology and medicine research since most biological reactions occur at surfaces and interfaces [1–3]. Controllable functionalization of the solid substrates' surfaces is critical for bioanalysis [4], including biosensing [5], enzymatic reaction [6,7], etc. Tailored surface properties such as tunable reactivity, biocompatibility, or wettability could be obtained by different approaches of surface modification, so that the design of biofunctional surface is of great interest in bioanalysis research [8–11].

Enzymes exhibit a number of features that make their use advantageous as compared with the conventional chemical catalysts. However, this is hampered by lack of stability and reusability. Compared to free enzyme in solution, the immobilized enzyme is more stable and resistant to the environmental changes by providing molecular level interactions with the substrates [12,13]. The main challenge is to develop a simple and general technique to engineer the surface for the immobilization of biomolecules. The layer-by-layer (LbL) technique is a facile method to engineer surface with targeted properties for the construction of biofunctional films [14–16]. The procedure is based on the alternative deposition of the oppositely charged polyelectrolyte [17], proteins [18], ceramics, or charged nanoparticles [19] on a charged surface by attractive electrostatic force. The functional surface made by alternate adsorption of charged nanoparticles and polyelectrolytes provides a route for extending three-dimensional "molecular" architecture in a direction perpendicular to the solid support [20]. This multilayer film maintains surface characteristics of nanoparticles and has good thermal and mechanical stability. Biomolecules embedded into such multilayer film could keep a secondary structure close to their native form, which is crucial to biological analysis [21].

* Corresponding authors. Tel.: +86 21 65642138; fax: +86 21 65641740.
E-mail addresses: zhangyh@fudan.edu.cn (Y. Zhang), bhliu@fudan.edu.cn (B. Liu).

1388-2481/$ - see front matter © 2007 Elsevier B.V. All rights reserved.
doi:10.1016/j.elecom.2007.02.018

Up to now, many advanced functional materials have been used to immobilize biomolecules on the solid substrates, such as mesoporous silicates, zeolites and polymers. With the development of nanotechnology, many nanomaterials [22] have been reported in the application for fabricating the functional surfaces due to their large surface area for biomolecular immobilization. Nanozeolites possess special surface properties, including large and clean surface without any protection or surface-modifying agent, adjustable surface charge and composition, and stable colloidal property in both aqueous and organic solutions, which make them suitable to fabricate functional surface for the immobilization of biomolecules.

We report herein a biocompatible interface composed by a beta-nanozeolite three-dimensional architecture on an indium tin oxide (ITO) electrode using LbL assembly technique. The large surface area and unique surface property of the nanozeolite matrix resulted in a high enzyme adsorption capacity, and the enzyme adsorbed in this film retained its activity to a large extent. Adjusting the nanozeolite-assembled layers, thus regulating the amount of the enzyme immobilized, could facilely control the biocatalytic property of the enzyme electrode. The amperometric response of the enzyme electrode was acquired to probe the trace phenol as proposed.

2. Experimental section

2.1. Reagents

Tyrosinase (from mushroom, EC 1.14.18.1, $M_r \sim 125\,000$) was purchased from Fluka. Poly (diallyldimethylammonium chloride) (PDDA, $M_w < 200\,000$), poly(sodium 4-styrenesulfonate) (PSS, $M_w \sim 70\,000$) were obtained from Aldrich. 3-mercapto-1-propanesulfonate (MPS, 90%) were purchased from Aldrich. All chemicals were of analytical grade and were used without further purification. All solutions were prepared with bidistilled water.

2.2. Construction of the tyrosinase/nanozeolite/ITO electrode

Colloidal crystals of beta-nanozeolite were synthesized in a mixture solution with the molar composition of $12(TEA)_2O{:}Al_2O_3{:}60SiO_2{:}588\ H_2O$ according to a literature method [23]. The obtained nanosized zeolites were purified by centrifugation and redispersion in a 0.1 M ammonia solution for three times. The last colloid was adjusted to a solid content of 1.0 wt% and pH 10 to make the zeolite nanoparticles stable and negatively charged. The ITO electrode was cleaned by sequentially sonication in acetone and distilled water, and then treated in a basic solution ($NH_4OH{:}H_2O_2{:}H_2O = 1{:}1{:}5$ in volume ratio). Nanozeolite modified ITO electrode was prepared by LbL assembly method: the pre-treated ITO electrode was coated with cationic PDDA solution and anionic PSS solution in the sequence of PDDA/PSS to provide a negatively charged surface. Afterwards, the electrodes were alternately incubated in PDDA solution and negatively charged nanozeolite solution for 30 min each. When this cycle procedure was repeated N times, the $(\text{nanozeolite/PDDA})_N$/ITO electrode was obtained. Tyrosinase immobilization was achieved by immersing this modified electrode in tyrosinase solution (1.0 mg mL^{-1}, 20 mM phosphate buffer solution, pH 6.0) at 277 K. Fig. 1 displays the schematic model for tyrosinase/$(\text{nanozeolite/PDDA})_N$ films on the ITO electrode.

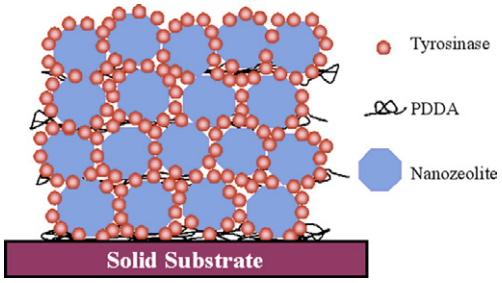

Fig. 1. Schematic diagram of tyrosinase/$(\text{nanozeolite/PDDA})_N$ film assembled on a solid substrate.

2.3. Quartz crystal microbalance measurements

The microgravimetric analysis was performed with Quartz crystal microbalance (QCM) analyzer (CHI440, CH Instruments, Shanghai, China) and quartz crystals (8 MHz) sandwiched between two Au electrodes (area 0.196 cm^2). The QCM resonator was cleaned in a mixed solution of H_2SO_4 and H_2O_2, followed by rinsing with bidistilled water and alcohol. Then the resonator was immersed into MPS solution to form a negatively charged surface. The assembly procedure of $(\text{nanozeolite/PDDA})_N$ multilayer films on QCM resonator was the same as that on ITO electrode. After each layer formed, the resonator was taken out, thoroughly rinsed with pure water and dried by N_2 blast, and then the frequency shift was measured. At last, immersed this modified resonator in tyrosinase solution (1.0 mg mL^{-1}, 20 mM phosphate buffer solution, pH 6.0) at 277 K, QCM measurement was made after rinsing and drying the resonator. The adsorbed mass of each layer was calculated with the Saurbrey equation [24]. Taking into account characteristics of the present resonators, the film mass per unit area M/A(g cm^{-2}) is given by the following equation: $M/A\ (\text{g cm}^{-2}) = -\Delta F(\text{Hz})/(1.45 \times 10^8)$.

2.4. Amperometric sensor measurements

The tyrosinase/$(\text{nanozeolite/PDDA})_N$/ITO sensor was immersed in a thermostated electrochemical glass cell containing 10 mL of 0.05 M phosphate buffer solution under different pH values (4.0–9.0) at 303 K. Under constant stirring, a current recording was started at a potential of −200 mV (versus SCE). The background current was

allowed to decay to a steady state before aliquots of phenol standard solution were added into the cell and the current-time curves were recorded. All the electrochemical experiments were performed in a three-electrode system consisting of a platinum foil counter electrode, a saturated calomel reference electrode (SCE), and the modified ITO working electrode. The electrochemical measurements were carried out on CHI 660A Electrochemical Workstation (CH Instrument, Shanghai, China).

3. Results and discussion

3.1. The assembly-controlled enzyme/nanozeolite films on the electrode surfaces

The beta-nanozeolite with a SiO_2/Al_2O_3 ratio of 43.8, a kind of alumino-silicate crystal type material, was hydrothermally prepared according to the literature [23]. SEM result depicted in Fig. 2A reveals that the prepared nanozeolites are about 80–100 nm in diameter with a narrow size distribution, whereas TEM image (Fig. 2B) proves their crystalline essence with an uneven surface morphology, which endows them with both the special surface property and the large external surface area that is desirable for biomolecular immobilization. Fig. 2C and D display the SEM images of the modified electrode with different nanozoelite assembly layers, which are named as (nanozeolite/PDDA)$_3$/ITO, (nanozeolite/PDDA)$_7$/ITO, respectively. It can be seen that the density and uniformity of the surface of modified electrodes are improved by the successive assembly procedure. Moreover, the effective spaces of the surface of modified electrodes for enzyme immobilization are enhanced by the increasing nanozeolite assembling cycles. Therefore, the LbL assembly technique for nanozeolite not only could broaden the efficient contact area and space between the enzyme molecules and the modified electrodes, but also could control the enzyme immobilization amount via its simple but recycling procedure.

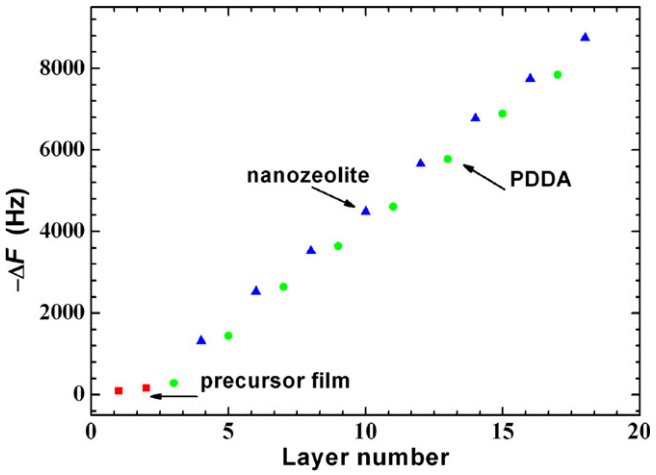

Fig. 3. QCM frequency shifts for cycles of alternate nanozeolite/PDDA assembly and first two steps PDDA/PSS assembly on gold resonator.

QCM measurements were used to monitor the alternate film assembly (Fig. 3) and the adsorption of enzymes on the electrodes with different nanozeolite-modified layers (Fig. 4). A precursor film consisting of polycation (PDDA)/polyanion (PSS) layers was primarily assembled on the electrode surface to offer a supporting cushion (Fig. 3, precursor film). As shown in Fig. 3, the regular stepwise frequency shifts indicated linear growth during the film assembly procedure with the increasing number of the nanozeolite films. According to the ΔF of each nanozeolite adsorption step, the mass of the nanozeolite assembled in each layer was calculated to be about 7.24 μg cm^{-2}. Fig. 4

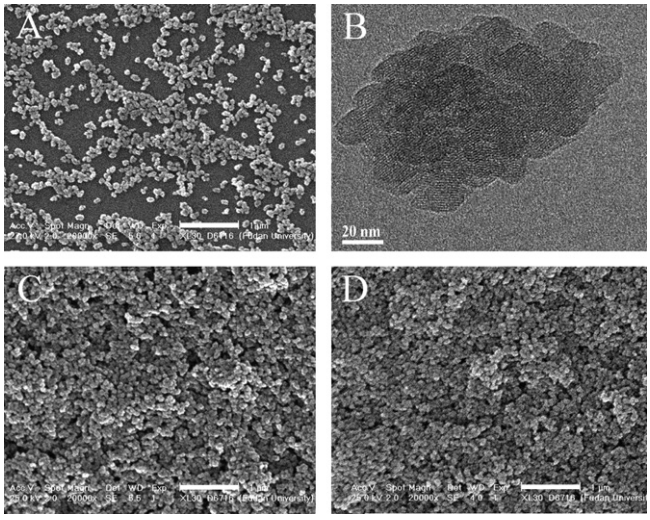

Fig. 2. Typical SEM image (A) and TEM image (B) of beta-nanozeolite particles; Representative SEM images of (nanozeolite/PDDA)$_3$/ITO (C), (nanozeolite/PDDA)$_7$/ITO (D) by LbL assembled. The bars in SEM images are 1 μm, and the bar in TEM image is 20 nm.

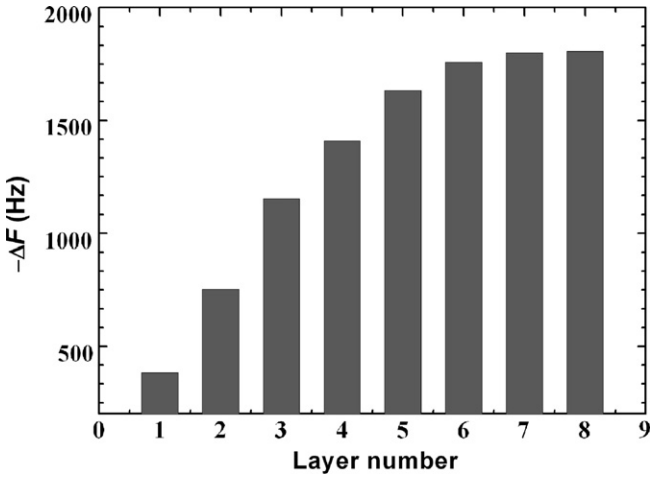

Fig. 4. QCM frequency shifts for the adsorption of tyrosinase (1.0 mg mL^{-1}) on the different (nanozeolite/PDDA)$_N$/ITO electrodes, respectively. N value represents assembled layer number of nanozeolite/PDDA bilayer.

shows the total QCM frequency shifts (ΔF) for tyrosinase adsorption on the different (nanozeolite/PDDA)$_N$/ITO electrodes. The ΔF was linear increase at first three bilayers ($N = 1,2,3$) and was gradually reaching saturation after seven bilayers. We speculate that the first three nanozeolite layers are within an incompact microenvironment, and enzymes can easily inhabit the active sites of the nanozeolite surface. As the number of layers increases, the denseness of surface is augmented and some sites suitable for enzyme adsorption are inaccessible due to the diffusion limitation. According to the experimental data, the amount of the tyrosinase immobilized on the (nanozeolite/PDDA)$_N$/ITO electrode reached 7.95 μg cm^{-2}, 11.26 μg cm^{-2} and 12.41 μg cm^{-2} for 3, 5 and 7 nanozeolite assembled layers, respectively. Combined with the amount of nanozeolites on these electrodes, it concluded that the nanozeolite matrix possessed a high adsorption amount (nearly 350 mg g^{-1} nanozeolite), which indicates that such well-assembled nanozeolite architecture is suitable for enzyme accomodation.

3.2. Amperometric response characteristics of tyrosinase/nanozeolite biosensor

The tyrosinase/(nanozeolite/PDDA)$_N$/ITO electrode was applied as a biosensor for the detection of phenol. Fig. 5 illustrates the typical current–time plots of the tyrosinase biosensors at pH 7.0. With the addition of phenol aliquot samples, the stepwise increase of the reduction current was detected and the response time with 95% steady-state response being achieved was less than 5 s. It was clearly shown that the sensitivity of tyrosinase/(nanozeolite/PDDA)$_N$/ITO was about 400 μA mM^{-1} for biosensor with 7 nanozeolite assembled layers (i.e., $N = 7$), which was 4-times higher than that with 3 nanozeolite assembled layers (i.e., $N = 3$). This amperometric response phenomena could be deduced from the QCM measurement results of enzyme adsorption on the modified resonator. The layer of assembled film changing from $N = 3$ to 7, the immobilized enzyme amount and amperometric response increased regularly, implying that the function of the enzyme electrodes could be controlled facilely through the LbL technique. In addition, the influence of pH (4.0–9.0) for the biosensor was studied, and it was found that the biosensor displayed an optimum response at pH values ranging from 6.6 to 7.4, which is consistent with the irreversible loss of activity below pH 4.5 and beyond pH 9.3 for free tyrosinase [25].

Fig. 6 shows the calibration curve of the tyrosinase/(nanozeolite/PDDA)$_7$/ITO biosensor. The linear response of the biosensor to phenol was from 1×10^{-8} M to 1.8×10^{-5} M with a correlation coefficient of 0.9995. The detection limit was 0.5 nM (shown in Fig. 6 inset). The apparent Michaelis–Menten constant K_M^{app} of tyrosinase/(nanozeolite/PDDA)$_7$/ITO biosensor was calculated to be 24 μM according to the Lineweaver–Burke type equation [26]. This value is similar to the previous reports for the tyrosinase biosensors based on a colloidal gold modified carbon paste electrode (53.6 ± 3.2 μM) [27], and carbon nanotube modified electrode (30 μM) [28]. Additionally, the biosensor displays a good operational stability and long-term stability. For example, the nanozeolite modified biosensor retains about 93% of its initial activity after 3 h successive performance. Even if it was stored for 10 weeks at 4 °C, 85% of its initial response could be kept yet. Such good performances of the biosensor might be attributed to the fact that the well-defined interface assembled by the nanozeolites provided the biocompatible microenvironment for enzyme immobilization, which is an important issue for the sensitive biosensor.

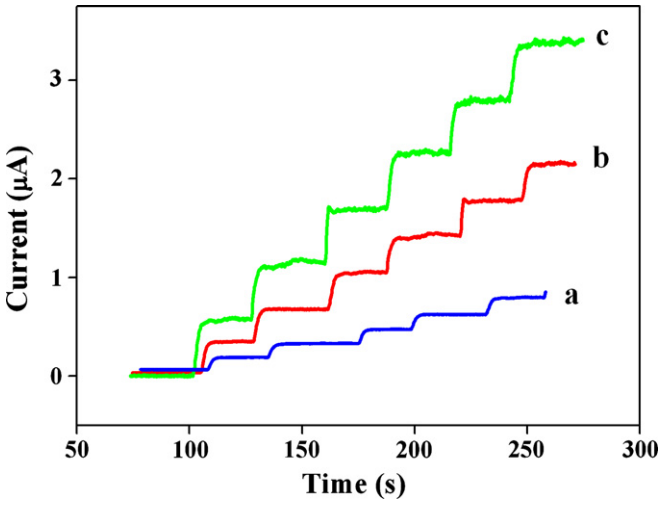

Fig. 5. Amperometric response of the tyrosinase/(nanozeolite/PDDA)$_N$/ITO electrode with $N = 3$ (a), 5 (b), 7 (c) at −200 mV (versus SCE) upon successive addition of 15 μL phenol solution (1 mM) to 10 mL phosphate buffer solution (50 mM) at pH = 7.0, respectively.

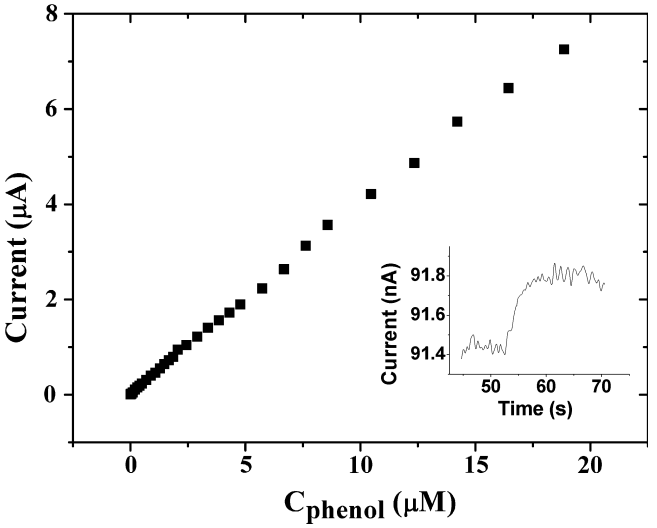

Fig. 6. Calibration curve of the tyrosinase/(nanozeolite/PDDA)$_7$/ITO sensor for phenol detection. Inset: amperometric response of the detection limit.

4. Conclusion

A stable nanozeolite film has been multilayer-assembled on the ITO surface by the alternating deposition of beta-nanozeolite and PDDA polycation. The tyrosinase biosensor based on this biocompatible surface showed a high sensitivity and a good long-term stability, which was attributed to the high immobilization capacity and the good biocompatibility of the nanozeolite-assembled layers for enzyme. Moreover, the function of the enzyme electrodes can be tailored by varying the number of bilayers deposited on the electrode surface, thus providing a simple way to control the enzyme immobilization and bioactivity for the purpose of biosensor. It is shown that the zeolite nanoparticles are promising candidates for biomolecular immobilization and the nanozeolite-modified surface could be widely applied in the biosensors, bioreactors and many other nanodevices.

Acknowledgement

This work was supported by National Natural Science Foundation of China (20575013, 20303003, 20421303), STCSM (05QMH1402, 05QMX1403, 05 nm05038, 05DJ14005, 06DJ14006), Shanghai Shuguang project and Perpignan University via a visit professor fellowship to BHL.

References

[1] Y. Lvov, Z. Lu, J.B. Schenkman, X. Zu, J.F. Rusling, J. Am. Chem. Soc. 120 (1998) 4073.
[2] B. Thierry, F.M. Winnik, Y. Merhi, M. Tabrizian, J. Am. Chem. Soc. 125 (2003) 7494.
[3] T. Groth, A. Lendlein, Angew. Chem. Int. Ed. 43 (2004) 926.
[4] R.J. Pei, X.Q. Cui, X.R. Yang, E.K. Wang, Biomacromolecules 2 (2001) 463.
[5] T. Yu, Y.H. Zhang, C.P. You, J.H. Zhuang, B. Wang, B.H. Liu, Y.J. Kang, Y. Tang, Chem. Eur. J. 12 (2006) 1137.
[6] Y. Liu, W. Zhong, S. Meng, J.L. Kong, H.J. Lu, P.Y. Yang, H.H. Girault, B.H. Liu, Chem. Eur. J. 12 (2006) 6585.
[7] Y.H. Zhang, Y. Liu, J.L. Kong, P.Y. Yang, Y. Tang, B.H. Liu, Small 2 (2006) 1170.
[8] G. Acharya, T. Kunitake, Langmuir 19 (2003) 2260.
[9] Z. Ademovic, A. Gonera, P. Mischnick, D. Klee, Biomacromolecules 7 (2006) 1429.
[10] X. Zhang, F. Shi, X. Yu, H. Liu, Y. Fu, Z.Q. Wang, L. Jiang, X.Y. Li, J. Am. Chem. Soc. 126 (2004) 3064.
[11] S.C. D'Andrea, A.Y. Fadeev, Langmuir 22 (2006) 3962.
[12] J. Deere, E. Magner, J.G. Wall, B.K. Hodnett, Chem. Commun. (2001) 465.
[13] A. Vinu, M. Miyahara, K. Ariga, J. Phys. Chem. B 109 (2005) 6436.
[14] Y. Lvov, G. Decher, H. Mohwald, Langmuir 9 (1993) 481.
[15] L. Wang, T. Sasaki, Y. Ebina, K. Kurashima, M. Watanabe, Chem. Mater. 14 (2002) 4827.
[16] W. Jin, X.Y. Shi, F. Caruso, J. Am. Chem. Soc. 123 (2001) 8121.
[17] G. Decher, Science 277 (1997) 1232.
[18] M.K. Beissenhirtz, F.W. Scheller, W.F.M. Stöcklein, D.G. Kurth, H. Möhwald, F. Lisdat, Angew. Chem. Int. Ed. 43 (2004) 4357.
[19] M.N. Zhang, Y.M. Yan, K.P. Gong, L.Q. Mao, Z.X. Guo, Y. Chen, Langmuir 20 (2004) 8781.
[20] Y. Lvov, B. Munge, O. Giraldo, I. Ichinose, S.L. Suib, J.F. Rusling, Langmuir 16 (2000) 8850.
[21] D.S. Salloum, J.B. Schlenoff, Biomacromolecules 5 (2004) 1089.
[22] S.H. Brewer, W.R. Glomm, M.C. Johnson, M.K. Knag, S. Franzen, Langmuir 21 (2005) 9303.
[23] M.A. Camblor, A. Corma, A. Mifsud, J. Perez-Pariente, S. Valencia, Stud. Surf. Sci. Catal. 105 (1997) 341.
[24] G. Sauerbrey, Z. Phys. 155 (1959) 206.
[25] Z.J. Liu, B.H. Liu, J.L. Kong, J.Q. Deng, Anal. Chem. 72 (2000) 4707.
[26] R.A. Kamin, G.S. Wilson, Anal. Chem. 52 (1980) 1198.
[27] S.Q. Liu, J.H. Yu, H.X. Ju, J. Electroanal. Chem. 540 (2003) 61.
[28] Q. Zhao, L.H. Guan, Z.N. Gu, Q.K. Zhuang, Electroanalysis 17 (2005) 85.